Single Photon Infrared Emission Spectroscopy of the Gas Phase Pyrene Cation: Support for a Polycyclic Aromatic Hydrocarbon Origin of the Unidentified Infrared Emission Bands

H.-S. Kim,* D. R. Wagner,† and R. J. Saykally‡

Department of Chemistry, University of California, Berkeley, California 94720

(Received 6 November 2000)

We report the first observation of infrared emission from a gaseous ionic polycyclic aromatic hydrocarbon (PAH), the pyrene cation, over the range of wavelengths spanned by the ubiquitous interstellar unidentified infrared emission bands (UIRs). The complete set of pyrene cation IR emissions is observed, with relative intensities consistent with astrophysical observations, supporting the proposal that ionized PAHs are major contributors to the UIR bands. Additionally, unidentified features possibly arising from dehydrogenated PAH species are noted in the spectrum.

DOI: 10.1103/PhysRevLett.86.5691 PACS numbers: 33.20.Ea, 95.85.Hp

The unidentified infrared emission bands (UIRs) are a set of prominent spectral features emitted by dusty interstellar objects immersed within high UV flux regions. Polycyclic aromatic hydrocarbon (PAH) molecules have been proposed as the carriers, which implies that these constitute a significant reservoir of carbon in the universe [1]. However, no explicit matches between laboratory IR emission spectra of PAHs and the UIRs have yet been convincingly demonstrated, except for the nonspecific 3.3 μm band [2–4]. Moreover, *neutral* PAHs cannot be the major contributors to the interstellar emissions because the relative intensities of their vibrational bands grossly disagree with those of the UIRs. Recent matrix isolation absorption spectroscopy experiments [5,6] and *ab initio* calculations [7,8] indicate that PAH *cations* exhibit a much more favorable spectral pattern, but the gas phase IR emission experiments needed to definitively evaluate their potential as UIR carriers have been technically prohibitive. Here, we report the first observation of gas phase IR emission spectra from PAH cations made by our recently developed infrared photon counting technique [3,4]. The measured spectrum of the pyrene cation ($C_{16}H_{10}^+$) agrees quite well with major UIR feature intensities (weak 3.3 μm band, strong 6–9 μm emission), thus providing support for the "PAH hypothesis."

Many astronomical studies have now firmly established that the five strong emission features (3.3, 6.2, 7.7, 8.6, and 11.3 μm), as well as a variety of minor bands, observed in infrared spectra of many objects both inside and outside of the Galaxy are characteristic of interstellar dust [9]. Establishing the chemical composition of the substances emitting these bands is an important problem because these must be very widespread and abundant. Despite much progress over two decades, a definitive assignment has not yet been realized. The currently favored candidates [1,6,9] for carriers of the UIRs are PAH cations (PAH^+), as the relative intensities of PAH^+ vibrational bands match those of the UIRs much better than do the corresponding bands of neutral PAHs, particularly in that the 3.3 μm (aromatic C—H stretch) band is much weaker than the 6–9 μm (C—H in-plane bend, C═C stretch) bands, whereas neutral PAHs exhibit a very strong 3.3 μm feature. However, due to the large matrix perturbations expected for ionic molecules, as well as the strong dependence of IR fluorescence on excitation energy, gas phase experiments are necessary to definitively test these proposals.

We have developed an infrared photon counting method based on a blocked impurity band solid state photomultiplier (BIB-SSPM) [10] for the purpose of measuring IR emission spectra of large molecules under conditions approximating those in the Interstellar Medium. We have recently used this new technique [3,4,11] (single photon infrared emission spectroscopy, SPIRES) to measure gas phase IR emission from a number of UV laser-excited neutral PAHs over the entire spectral range of the UIRs. Apart from the 3.3 μm feature, no acceptable matches with UIR features were found. Here, we describe the extension of SPIRES to PAH cations, generated and observed in a well-characterized ion beam.

Experimental.—The Berkeley SPIRES has been described in detail elsewhere [3,4]. It consists of a liquid-helium-cooled 0.48-m focal length Czerney-Turner monochromator containing a ten-element array As:Si blocked impurity band solid state photomultiplier (BIB-SSPM, Rockwell Inc. [10]). It was interfaced with an ion beam apparatus for the present study. The ion beam system (Fig. 1) consists of an ion source, a series of electrostatic lenses, a quadrupole deflector, and a reflectron.

A number of technological barriers were surmounted to make this experiment possible. IR emission is an inherently weak process, typically demanding a high concentration of emitters, while the high-current ion beam system had to accommodate the stringent demands (saturation count ~10^7 photons/second) of the ultrasensitive IR detector. The ionizer and extractor used in this work are similar to standard designs published elsewhere [12]. We employ a modified nude ionization gauge (Varian UHV-24) with a dual tungsten filament with the top end of the thin-grid cage removed to make space for the extraction electrode. Pyrene is vaporized from a

© 2001 The American Physical Society

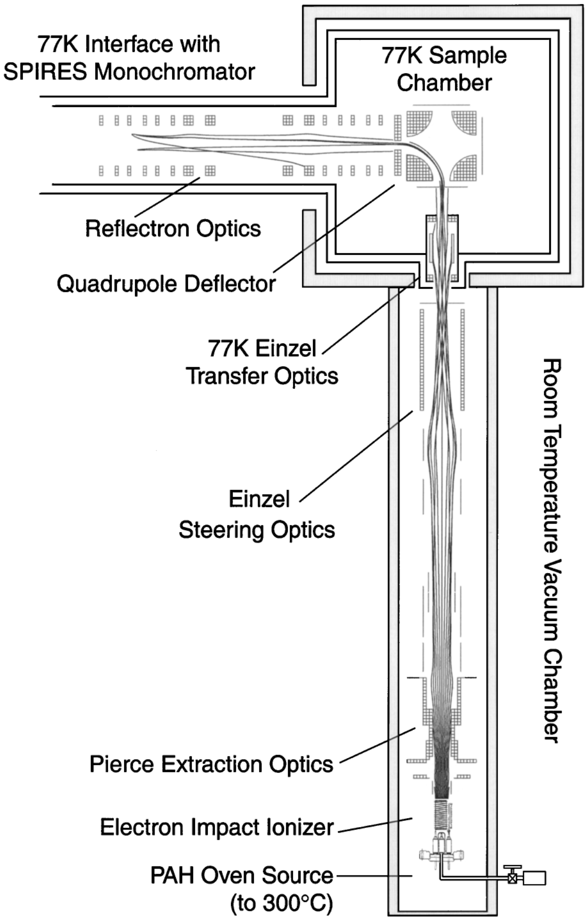

FIG. 1. PAH ion beam schematic: Pure PAH is vaporized in a resistively heated oven, and the PAH vapor is introduced into the back side of the ionizer via stainless steel tubing. Ions resulting from 80 eV electron impact follow a trajectory defined by the ion optics. One such trajectory (Simion ion trajectory simulation) is shown, wherein the ions are extracted, focused through small apertures into the cryogenic sample chamber, and steered into the viewing region of the SPIRES monochromator with a quadrupole deflector. The final reflection region decelerates the ions, and returns them back toward the sample chamber, effectively increasing their residence time, during which the ions radiate excess vibrational energy (acquired from electron impact) as IR photons detected by the SPIRES spectrometer. The background signal is collected when the ions are deflected out of the beam path before entering the viewing region.

crystalline solid (99%, Aldrich) at 70 °C, and introduced through the hole in the back of the ionizer left by removal of the ionization gauge collector. 80 eV electrons produce primarily monocationic pyrene ($C_{16}H_{10}{}^{+}$) due to the high activation energies required for fragmentation [13].

PAH ions are extracted from the ionizer and accelerated/focused with room temperature electrostatic optics into the entrance aperture of the cryogenic transfer (Einzel) lens, which refocuses the ions into the entrance aperture of a quadrupole deflector. The use of small apertures reduces the gas load of the sample chamber as well as the blackbody radiation admitted into the field-of-view of the monochromator. The quadrupole deflector, mounted onto the inner shield of our sample chamber cryostat, turns the ion beam 90° into the field-of-view of the liquid helium cooled SPIRES monochromator. The transfer optics, deflector, and reflectron were held at 77 K, which enabled us to acquire SPIRES data to wavelengths as long as 12 μm before the blackbody background saturated the detector.

The ion beam travels directly towards the monochromator entrance slit, and then is either reflected at the entrance of the monochromator by the reflectron field, or deflected into a Faraday cup where the ion current is measured. The reflectron field protects the monochromator optics from being deposited with PAHs and increases the time interval during which the IR fluorescence can be detected. The total ion current measured in the viewing region exceeded 2 μA at 1 keV ($>10^6$ pyrene$^+$/cm^3).

We used a 150 grooves/mm grating for spectral regions from 2.4 to 4.0 μm, 75 grooves/mm in regions from 5.5 to 9.2 μm, and 50 grooves/mm in regions from 9.5 to 12.0 μm. The relative intensities of features measured with the same grating are accurately determined, whereas intensity comparisons of features measured with different gratings (corrected for the instrument response) are somewhat less reliable. The SPIRES bands of the pyrene cation, observed from 2 to 12 μm, are summarized in Table I and shown in Fig. 2.

Results and discussion.—The SPIRES spectrum in Fig. 2(b) was obtained when the ions generated by electron impact of pyrene vapor were injected into the reflectron region. The general features of the IR spectra of pyrene cation are substantially different from those of neutral pyrene, studied in our previous SPIRES experiments and shown in Fig. 2(a) for comparison. Specifically, the C—H stretch near 3.3 μm is very weak, and the IR intensities of some bands in the 6–10 μm region (C=C stretch and C—H in-plane bend) are much stronger than those of the bands observed above ~10 μm (C—H out-of-plane bend). Torii *et al.* have discussed the vibronic interactions that give rise to these intensity differences between neutral and cationic PAHs [14].

Under the same conditions, the background spectrum in Fig. 2(c) was obtained when the ions were deflected before entering the monochromator field-of-view. The background spectrum is essentially flat over the spectral range studied. If collision induced dissociation and/or ion-electron recombination occurred exclusively in the reflectron region, then the spectrum 2(b) could include the IR emission from neutrals or fragment ions, but this seems unlikely. Hence, the observed spectrum is attributed to ionic species.

Electron impact of pyrene vapor is known to generate dehydrogenated pyrene cations ($C_{16}H_9{}^{+}, C_{16}H_8{}^{+}$), and pyrene dication ($C_{16}H_{10}{}^{2+}$) as well as parent pyrene cation ($C_{16}H_{10}{}^{+}$). According to mass spectral intensities [13], the molar ratios of cations generated by electron impact of pyrene are approximately $C_{16}H_{10}{}^{+}:C_{16}H_9{}^{+}:C_{16}H_8{}^{+}:$

TABLE I. Pyrene cation features observed by theory, matrix isolation, and the SPIRES infrared emission techniques. Unidentified features are most likely due to doubly dehydrogenated, doubly ionized, or protonated pyrene cation.

Pyrene cation						Unidentified features	
Theory (4-31G/DFT)		Matrix[a]		SPIRES (this work)			
λ (μm)	Rel. int.	λ (μm)	Rel. int.	λ (μm)	Rel. int.	λ (μm)	Rel. int.
3.24	0.03			3.34	0.01	2.64	(0.04)
6.52	**1.00**	6.45	**1.00**	6.51	**1.00**	2.97	(0.03)
		6.44				3.34	(0.01)
6.98	0.16	6.94	0.07	6.96	0.28	3.54	(0.04)
7.08	0.10	7.04	0.12	7.06	0.20	3.80	(0.12)
7.47	0.70	7.34	0.35	7.56	0.12	6.82	(0.16)
		7.36		7.71[b]	0.38	5.83	(0.06)
7.99	0.47	8.03	0.44	7.97	0.29	5.98	(0.29)
8.20	0.09	8.22	0.10	8.20	0.15	7.15	(0.47)
9.10	0.05	9.07	0.07	8.90	0.17	7.43	(0.09)
10.4	0.06	10.3	0.05			8.03	(0.37)
11.6	0.58	11.6	0.39	11.83	0.35	8.82	(0.20)
14.6	0.24	14.5	0.19				

[a] Some of the weak matrix bands have been excluded for clarity.

[b] No matrix or theory analogs for this feature are known; however, the intensity of this feature is similar to those between 7.3–7.5 μm in those studies and, hence, may be related.

$C_{16}H_{10}^{2+}$: $C_{16}H_8^{2+}$ ≅ 1.0:0.14:0.2:0.1:0.08. Several currently unassigned bands reported here may relate to these species. However, the major features observed in the SPIRES spectrum of pyrene agree very well with both cryogenic matrix IR spectra [5,6] and *ab initio* vibrational bands [8] of the pyrene cation, as shown in Table I and Fig. 3. In terms of relative intensities, SPIRES bands at 6.51(1.00), 6.96(0.28), 7.06(0.20), 7.56(0.12) or 7.71(0.38), 7.97(0.29), 8.20(0.15), 8.90(0.17), and 11.83(0.35) μm in Fig. 2 correspond to those at 6.44 ~ 6.45(1.00), 6.94(0.07), 7.04(0.12), 7.34 ~ 7.36(0.35), 8.03(0.44), 8.22(0.10), 9.07(0.07), and 11.61(0.39) μm in the matrix spectra [5]. The strongest band observed in our spectrum (6.51 μm) shows a 15 ~ 20 cm^{-1} redshift relative to bands measured in cryogenic matrix absorption experiments (6.44 ~ 6.45 μm). Similar redshifts due to high internal energy content were also observed in our previous IR emission spectra of neutral PAHs [4]. The C=C stretching modes (6.51 − 7.71 μm) and the out-of-plane bending mode at 11.83μm also show redshifts, but in-plane bending modes (7.97–8.90 μm) exhibit blueshifts relative to the matrix results. The combined effects of the matrix shifts and shifts due to high vibrational energy of the PAH emitters are not yet well characterized for PAH ions, and such correlations are essential for a proper comparison of matrix data to the UIRs.

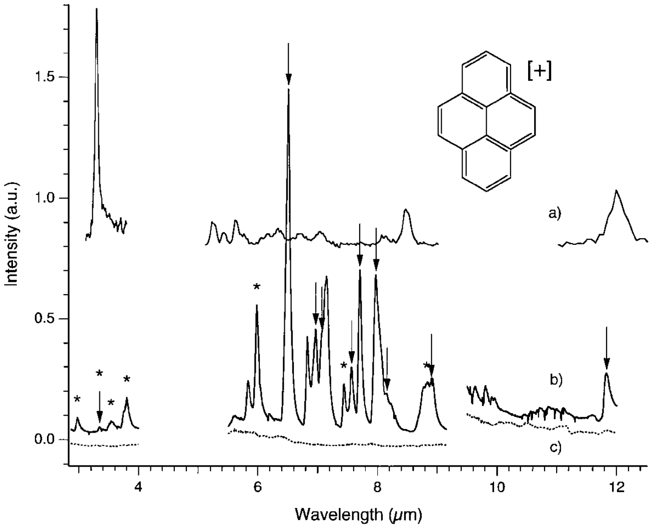

FIG. 2. SPIRES spectrum of the pyrene cation: Trace (a) is the gas phase SPIRES spectrum of neutral pyrene reported previously [3] and shown for comparison. Note the 3.3 μm band is the dominant feature in the spectrum and extends off scale. Peaks attributed to the pyrene cation ($C_{16}H_{10}^+$) in trace (b) are denoted with arrows. Here, the dominant features of the spectrum occur in the 6–9 μm region, while the aromatic C—H stretch at 3.3 μm has nearly disappeared, consistent with theoretical predictions (see text). Features tentatively assigned to the doubly dehydrogenated pyrene cation ($C_{16}H_8^+$) are labeled with an asterisk. Unlabeled peaks are not currently identified. The background scan in trace (c) indicates that the IR emission observed in (b) is due to gas phase PAH ions.

Pauzat *et al.* calculated the IR frequencies and integrated intensities [15] for two isomers of doubly dehydrogenated pyrene cation ($C_{16}H_8^+$). The number of bands predicted to occur in this region generally supports the notion that the weaker features in the SPIRES spectra in Fig. 2(b) are due to the doubly dehydrogenated pyrene cation, but definitive assignments are not possible at this time. Additionally, Le Page *et al.* [16] reports that the reaction between the pyrene cation and hydrogen atoms proceeds to generate protonated pyrene cation ($C_{16}H_{11}^+$), which is more stable than either the pyrene cation or the

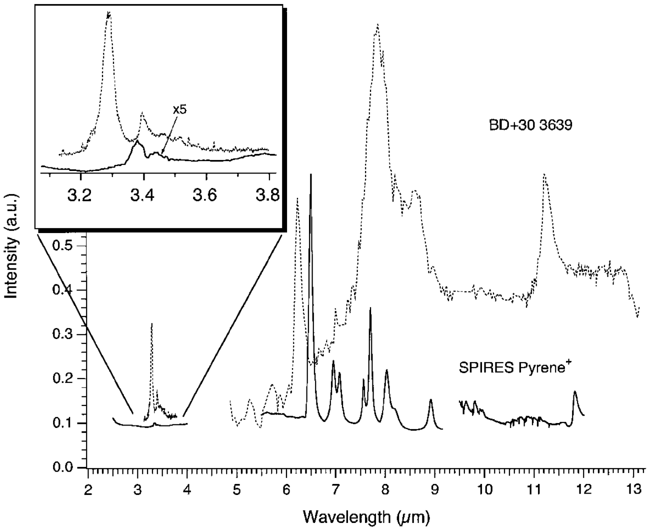

FIG. 3. SPIRES pyrene cation spectrum (lower trace) and UIR spectrum from BD30 + 3639: While the spectral details do not match exactly, the good general agreement of the positions and intensities of the pyrene cation emission spectrum with the UIR features supports the view that cationic PAHs are viable candidates for the UIR carriers. In order to definitively assess the contributions of a particular PAH^+ to the UIR bands, the internal energy content must be specified, since spectral positions and widths depend strongly on this property. This is not currently possible.

dehydrogenated pyrene cation with respect to collisional dissociation. The SPIRES data presented here may thus include such relatively uncharacterized species such as doubly ionized, protonated, and doubly dehydrogenated pyrene cation, but the dominant features are clearly due to the pyrene monocation and include all the known spectral features identified both in cryogenic matrix experiments and theoretical calculations.

The IR emission spectrum of the pyrene cation resembles the UIR features at 6.2, 7.7, 8.6, and 11.3 μm more closely than do those of any other PAHs examined in detail thus far [2–4] (see Fig. 3). Hence, the pyrene cation, and quite probably other PAH ions which are predicted to exhibit similar vibrational intensity patterns [8], can indeed be considered as viable candidates for carriers of the UIRs, in that the overall intensity patterns are similar. There is still not an exact agreement in the spectral positions, but these shift and broaden as a function of internal energy content, and this quantity is still not well-characterized in the SPIRES ion beam experiment. Additionally, recent results from matrix absorption spectroscopy [17] show that the C—H in-plane bend and the 7.7 μm C═C stretch band positions follow a trend toward UIR values with increasing molecular size. PAH ions with 50–80 carbon atoms may therefore better match the UIR features with respect to *both* band intensities and positions, but further studies are necessary to firmly establish this important conclusion.

This work was funded by the National Aeronautics and Space Administration Astrophysics (Grant No. NAG5-4521) and Exobiology (Grant No. NAG5-7457) programs. H.-S. K. would like to thank the Korea Research Foundation.

---

*Current address: Catalysis Center, Northwestern University, Evanston, IL 60208.

†Current address: Silicon Light Machines, 385 Moffett Park Drive, Sunnyvale, CA 94089.

‡Author to whom correspondence should be addressed. Email address: saykally@uclink.berkeley.edu

[1] L. J. Allamandola, A. G. G. M. Tielens, and J. R. Barker, Astrophys. J. **290**, L25–L28 (1985).
[2] S. Schlemmer *et al.,* Science **265**, 1686–1689 (1994).
[3] D. J. Cook *et al.,* Nature (London) **380**, 227–229 (1996).
[4] D. J. Cook *et al.,* J. Phys. Chem. A **102**, 1465–1481 (1998).
[5] M. Vala *et al.,* J. Phys. Chem. **98**, 9187–9196 (1994).
[6] D. M. Hudgins and L. J. Allamandola, J. Phys. Chem. **99**, 3033–3046 (1995).
[7] J. Szczepanski and M. Vala, Astrophys. J. **414**, 646–655 (1993).
[8] S. R. Langhoff, J. Phys. Chem. **100**, 2819–2841 (1996).
[9] L. J. Allamandola, A. G. G. M. Tielens, and J. R. Barker, Astrophys. J. Suppl. Ser. **71**, 733–775 (1989).
[10] M. D. Petroff, M. G. Stapelbroek, and W. A. Kleinhans, Appl. Phys. Lett. **51**, 406–408 (1987).
[11] D. R. Wagner, H.-S. Kim, and R. J. Saykally, Astrophys. J. **545**, 854–860 (2000).
[12] J. Kirschner, Rev. Sci. Instrum. **57**, 2640–2642 (1986).
[13] NIST website, www.nist.gov.
[14] H. Torii *et al.,* J. Phys. Chem. A **103**, 5557–5566 (1999).
[15] F. Pauzat, D. Talbi, and Y. Ellinger, Astron. Astrophys. **319**, 318–330 (1997).
[16] V. Le Page *et al.,* Int. J. Mass Spectrom. **187**, 949–959 (1999).
[17] D. M. Hudgins and L. J. Allamandola, Astrophys. J. Lett. **513**, L69–L73 (1999).